

## A Combined Approach for Predicting Binding Affinity of Zika Virus NS2B-NS3 Protease Inhibitors Using Semi-Empirical Methods and Molecular Docking Algorithms

Maycon Vinicius D. de Oliveira,<sup>id</sup><sup>a</sup> Leonardo L. Almeida,<sup>id</sup><sup>a</sup> João A. P. da Rocha,<sup>id</sup><sup>a,b</sup>  
Ana Lucia M. Wanzeller<sup>id</sup><sup>c</sup> and Anderson H. Lima<sup>id</sup>\*,<sup>a</sup>

<sup>a</sup>Laboratório de Planejamento e Desenvolvimento de Fármacos, Instituto de Ciências Exatas e Naturais, Universidade Federal do Pará, 66075-110 Belém-PA, Brazil

<sup>b</sup>Instituto Federal de Educação, Ciência e Tecnologia do Pará, Campus Bragança, 68600-000 Bragança-PA, Brazil

<sup>c</sup>Seção de Arbovirologia e Febres Hemorrágicas, Instituto Evandro Chagas, Ministério da Saúde, Secretaria de Vigilância em Saúde e Ambiente, 66093-020 Ananindeua-PA, Brazil

Zika virus (ZIKV) is a mosquito-borne virus that has emerged as a major public health concern due to its association with severe neurological disorders. In recent years, there has been increasing interest in exploring natural products as potential therapeutics for ZIKV infection. This study aimed to predict the binding affinity of natural compounds to the ZIKV NS2B-NS3 protease (NS2B-NS3pro) using multiple molecular docking algorithms and semiempirical quantum mechanical methods. Our results demonstrate that semiempirical methods can improve the accuracy of molecular docking studies for natural compounds. In this particular case, the PM7 (Parametric Method Number 7) method showed a significant improvement in the coefficient of determination ( $R^2 = 0.85$ ). We expect this combined approach to aid in the development of natural product-based therapies for ZIKV infection and to highlight the importance of continued research in this field.

**Keywords:** ZIKV, NS2B-NS3 protease, docking molecular, PM7, edible plants

### Introduction

The Zika virus (ZIKV) is a type of flavivirus, like Dengue, Yellow Fever, Chikungunya, and West Nile Fever (WNV). It is transmitted through the bite of mosquitoes of the genus *Aedes* and via human fluids such as semen and blood transfusions. It has been discovered that there are links between ZIKV and neurological diseases such as microcephaly (in newborns of women infected during pregnancy) and Guillain-Barre syndrome (in adults), as well as male infertility.<sup>1-4</sup> Additionally, human contact with this virus can also lead to more severe future cases of Dengue<sup>5</sup> and the lack of vaccines or effective treatments, coupled with the challenge of detecting Zika virus due to the similarity of its symptoms with other diseases, makes the prevention of mosquito proliferation the primary form of prophylaxis.<sup>6,7</sup>

The virus genome produces several non-structural proteins that play a crucial role in the evasion and

replication of ZIKV. These proteins could be potential targets for antiviral drugs. For instance, NS2B and NS3 proteins exhibit enzymatic activity only when they form a complex called Flavirin.<sup>7,8</sup> Hence, understanding the inhibition mechanisms of this complex is essential in the study of ZIKV. Roy *et al.*<sup>7</sup> discovered that six chemical compounds found naturally in edible plants, such as myricetin, quercetin, luteolin, isorhamnetin, apigenin, and curcumin, act as enzyme inhibitors of the NS2B-NS3Pro protein. These inhibitors are present in plants such as caper, tea, red onion, celery, broccoli, green pepper and turmeric.<sup>7</sup>

Recently, we have discussed computational approaches and methods developed to explore the chemo-structural diversity of natural products placing particular emphasis on artificial intelligence, cheminformatics methods, and big data analyses.<sup>9</sup> In this work, we aimed to address the critical challenge of accurately predicting the binding energies and conformations of this class of compounds that are crucial in drug discovery. Therefore, we utilized a combination of molecular docking algorithms and semiempirical quantum mechanical methods to predict the affinity of the six

\*e-mail: anderson@ufpa.br

Editor handled this article: Paula Homem-de-Mello (Associate)



natural compounds mentioned above. Our approach not only demonstrated that the use of semiempirical methods significantly improved the accuracy of binding energy calculations, but also provided valuable insights into the development of new drugs for treating Zika virus and potentially other flaviviruses.

## Methodology

### Preparing the molecular target and ligands for computational analysis

The structure of NS2B-NS3pro was obtained from the Protein Database (PDB)<sup>10</sup> (PDB ID: 6KK6).<sup>8</sup> To assess the amino acid sequence, we utilized the Chimera program (version 1.15)<sup>11</sup> for visual inspection of the three-dimensional structure. The compound named DV0 (in this work named LIG-00) was found in the active site of the NS2B-NS3pro complex, and its spatial coordinates served as a reference for the six compounds investigated in this study. The compounds shown in Figure 1 were optimized in Gaussian09 program<sup>12</sup> using the Hartree-Fock method with the 6-31G\* basis set. On the other hand, for protein preparation, we used the H<sup>++</sup> online free server (version 3.0)<sup>13</sup> to obtain the protonation states of the ionizable residues by pK<sub>a</sub> calculation at neutral pH.

### Prediction of the binding mode of natural compounds in the active site of ZIKV NS2B-NS3 protease

In this study, we employed three different docking tools to analyze the six natural compounds (Figure 1) against the NS2B-NS3pro enzyme: Molegro Virtual Docker (MVD),<sup>14</sup> AutoDock4 (AD4)<sup>15</sup> and CSD-GOLD.<sup>16</sup> The scoring functions utilized in each program are specified in Table 1. A total of 10 conformations for each ligand were generated using each software, resulting in a total of 180 conformations. The size of the grid (coupling area in sphere for MVD and Gold software, or box format for AD4) was selected based on the settings of each program and the size of the ligands.

The coordinates of the reference ligand (LIG-00) (PDB ID: 6KK6) in the active site of the NS2B-NS3Pro complex from ZIKV were used as a starting point for carrying out

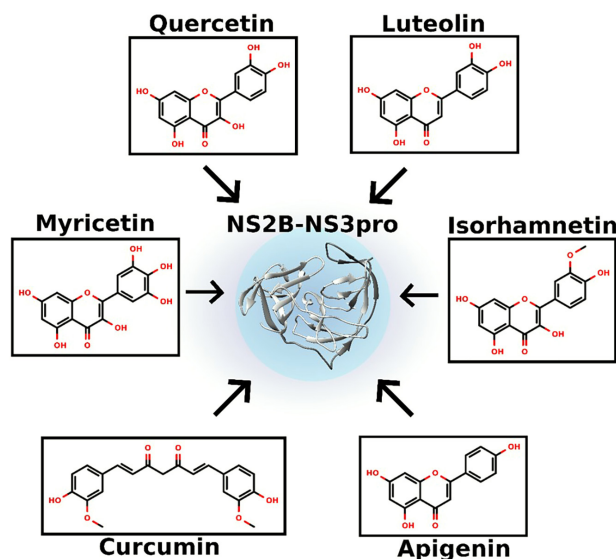


**Figure 1.** The 2D structures of the compounds that inhibit NS2B-NS3pro: myricetin, quercetin, luteolin, isorhamnetin, apigenin, and curcumin.

the molecular docking where  $X = 4.45 \text{ \AA}$ ,  $Y = -12.14 \text{ \AA}$ ,  $Z = 2.82 \text{ \AA}$ . Then, the conformations obtained with the lowest energies, for each molecule and software, were reserved for further analysis.

The experimental binding energies of the ligands were obtained using the inhibitor constant ( $K_i$ ) values<sup>7</sup> presented in Table 2.

In order to prove the molecular docking tools used in this work, redocking was performed using LIG-00 as a reference ligand at the NS2B-NS3Pro active site using grid size with  $10 \text{ \AA}$  in MVD,  $26, 26, 26 \text{ \AA}$  in AD4 ( $X, Y, Z$  grid size) and  $10 \text{ \AA}$  in GOLD. Thus, we conjecture that root mean square deviation (RMSD) needs to be less than or equal to  $1.0 \text{ \AA}$  to be considered satisfactory for replicating the ligand binding mode in the active binding site of NS2B-NS3Pro.<sup>17-19</sup> The grid measurements were adjusted, if necessary, to fit the size of the ligands and to provide greater flexibility according to the molecule structure.

### Reevaluating binding energies of the protein-ligand complexes

In the most recent versions of the chemical software MOPAC,<sup>20</sup> a module called MOZYME<sup>21</sup> was developed to be responsible for calculating the characteristics of protein-

**Table 1.** Molecular docking software, score function and the grid size ( $X, Y, Z$ )

Software	Score function	Grid size ( $X, Y, Z$ ) / $\text{\AA}$
Molegro Virtual Docker (MVD)	MolDock Score	10
Autodock 4.2 (AD4)	Lamarckian Genetic Algorithm and Empirical Free Energy	18, 18, 18
CSD-GOLD (GOLD)	ChemPLP (Score) and ASP (Rescore)	7

**Table 2.** ZIKV NS2B-NS3Pro  $K_i$  values for each ligand and its usual name

Ligand ID	Usual name	$K_i / \mu\text{M}$
01	myricetin	$0.8 \pm 0.1$
02	quercetin	$1.1 \pm 0.1$
03	luteolin	$1.4 \pm 0.1$
04	isorhamnetin	$6.2 \pm 0.4$
05	apigenin	$34.0 \pm 2.4$
06	curcumin	$2.6 \pm 0.2$

$K_i$ : inhibitor constant.

ligand complexes, which includes PM7<sup>22</sup> and some versions of PM6,<sup>23</sup> in systems above 18,000 atoms.<sup>24</sup>

Regarding the docking methods, the energy of protein-ligand binding is determined using force fields to describe molecular geometry. Sulimov *et al.*<sup>24</sup> found that semiempirical methods, specifically PM7, can improve the accuracy of ligand positioning and energy calculations. Therefore, the enthalpies of formation ( $\Delta H_f$ ) were calculated using MOPAC, and optimization of all atoms was performed using PM7 with the MOZYME module and implicit solvation. The energies were used to recalculate the binding energies of protein-ligand complexes. The keywords used in the calculations are described in Table 3.

**Table 3.** Keywords used in MOPAC2016 to determine enthalpies of formation

$\Delta H_f$	Keywords
Ligands	PM7 PRECISE AUX LARGE CHARGE=(X) SINGLET OPT GNORM=0.01 OPT ISCF EPS=78.4
Protein	PM7 PRECISE CHARGE=(X) LET T=1D ISCF MOZYME OPT GNORM=5 OPT PL XYZ EPS=78.4 RSOLV=1.3
Complex protein-ligand	PM7 PRECISE CHARGE=(X) LET T=1D ISCF MOZYME OPT GNORM=5 OPT PL XYZ EPS=78.4 RSOLV=1.3

$\Delta H_f$ : enthalpy of formation.

Finally, the selected conformations obtained from the molecular docking and PM7/MOPAC method (energy values in  $\text{kcal mol}^{-1}$ ) were used for consensus docking. The conformations were evaluated first by the software MVD,<sup>14</sup> AD4,<sup>15</sup> and GOLD.<sup>16</sup> For this, as in previous studies,<sup>17,18</sup> the following equation 1 was used.

$$X_{\text{software}} = \frac{X - X_{\text{min}}}{X_{\text{max}} - X_{\text{min}}} \quad (1)$$

where  $X_{\text{software}}$  is the factor referring to the docked ligand by the software in question, X is the value of binding energy

obtained in the docking of the specified ligand,  $X_{\text{min}}$  is the value of the lowest energy protein-ligand complex and  $X_{\text{max}}$  is the value of the lowest energy complex. Finally, the  $X_{\text{software}}$  values of each of the ligands, by software, were added in order to obtain the final ranking ( $F_r$ ) of the consensus (equation 2).

$$F_r = X_{\text{software(MVD)}} + X_{\text{software(AD4)}} + X_{\text{software(GOLD)}} \quad (2)$$

## Results and Discussion

Analysis of the docking scores between NS2B-NS3Pro and the ligands

Natural products are a rich source of potential drug candidates, but their structural complexity and diversity often present challenges in molecular docking studies. Obtaining accurate docking poses for natural compounds can be a difficult task.<sup>25,26</sup> In this study, we combined the use of multiple molecular docking algorithms and semi-empirical quantum computational methods to predict the binding affinity of six natural compounds to the NS2B-NS3 protease of ZIKV.

The best molecule according to the docking results (Table 4) was curcumin (06), with binding values of  $-117.5$  and  $-61.4 \text{ kcal mol}^{-1}$  using the MVD and GOLD scores, respectively. However, for the AD4 program, luteolin (03) had the best score ( $-6.85 \text{ kcal mol}^{-1}$ ). The molecular docking results were further optimized using the PM7 semiempirical method through the MOPAC 2016. After optimization, myricetin (01) showed the best energy value with  $-45.7$  and  $-29.7 \text{ kcal mol}^{-1}$  using binding modes obtained from MVD and AD4, respectively. This result supports the fact that myricetin has the lowest  $K_i$  value of  $0.8 \pm 0.1 \mu\text{M}$  (Table 4).

LIG-00 (from PDB 6KK6) was used as a reference (00) and presented the best score and energy values since it has the best experimental binding free energy value ( $-10.56 \text{ kcal mol}^{-1}$ ). By redocking LIG-00 at the active site of NS2B-NS3pro, we defined parameters to be used for similar molecules in this study. RMSD of redocking poses compared to crystal structure are 0.22, 0.86 and  $0.47 \text{ \AA}$  computed using MVD, AD4 and GOLD, respectively. Figure 2 shows the superimposition of the structures from redocking calculations.

Afterward, we used linear regression analysis to evaluate the improvement of molecular docking results by employing the PM7 method in comparison to the  $\Delta G_{\text{bind,exp}}$  obtained from the  $K_i$ .<sup>7</sup> Our results showed that PM7 method is an effective alternative for refining molecular docking results for those compounds, as evidenced by the linear regression presented in Figure 3.

**Table 4.** Binding energy values, obtained experimentally,<sup>7</sup> by molecular docking and by reoptimization using the semiempirical PM7 method

Ligand ID	$\Delta G_{\text{bind,exp}} /$ (kcal mol <sup>-1</sup> )	Docking score / (kcal mol <sup>-1</sup> )			$E_{\text{bind,PM7}} /$ (kcal mol <sup>-1</sup> )		
		MVD	AD4	GOLD	MVD	AD4	GOLD
01	-8.32	-100.9	-4.10	-41.4	-45.7	-10.1	-29.7
02	-8.13	-97.2	-3.86	-47.3	-24.7	-20.6	-15.6
03	-7.99	-95.7	-6.85	-49.8	-17.0	-9.28	-6.94
04	-7.10	-98.4	-6.02	-47.5	-20.0	-7.59	-12.4
05	-6.10	-92.2	-6.42	-49.5	-21.6	-5.97	-9.74
06	-7.62	-117.5	-3.07	-61.4	-21.0	-19.4	-6.83
00	-10.56	-186.6	-9.18	-73.1	-100.5	-49.7	-41.0

$\Delta G_{\text{bind,exp}}$ : binding energy value obtained experimentally by literature;  $E_{\text{bind,PM7}}$ : binding energy obtained by PM7 method; MVD: Molegro Virtual Docking; AD4: AutoDock 4; GOLD: CSD-GOLD.

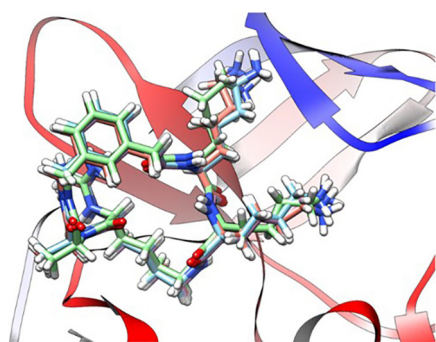


**Figure 2.** Best poses of each software obtained in redocking. Structures shown in lilac (MVD), green (AD4) and pink (GOLD) were compared to the reference ligand (light blue).

Using AD4 binding modes we have obtained an improvement in coefficient of determination ( $R^2$ ) values from 19 to 78% after optimization with PM7. GOLD results increased to 67% after the optimization while MVD showed a slight improvement of 3%.

It is worth noting that semiempirical methods have been used to enhance docking accuracy in molecular docking studies.<sup>27</sup> These methods can improve the calculation of electrostatic interactions between the ligand and protein, and lead to more accurate predictions of binding affinity and binding modes. However, it should be noted that the use of semiempirical methods is not always necessary or optimal for improving docking accuracy. The choice of method depends on the specific docking problem and the available computational resources. Rocha and Sant'Anna<sup>28</sup> proposed a methodology for investigating Shp2-selective inhibitors by combining docking and PM7 semi-empirical calculations. Our study presents a similar strategy, which is consistent with their approach. Both studies propose that this method has great potential for practical applications such as virtual screening, facilitating the rapid and efficient identification of potential inhibitors by researchers. Therefore, while our study suggests that the PM7 method can effectively refine molecular docking results, the

findings should be considered in light of other studies that report varying results with this method.

Analyses of the interactions between NS2B-NS3Pro and ligands in the active site

Using the proteins plus free web server<sup>29,30</sup> in analyzing PDB ID 6KK6 we obtained the diagram of intermolecular interactions with the reference inhibitor (LIG-00). We can observe that the main interactions that ligand 00 performs at the site are with the residues Asp83, Phe84, Asp129, Ala132, Asn152, Gly151, Gly153, Gly159, Tyr161 as shown in 2D-diagram<sup>31,32</sup> (Figure 4).

The molecular docking method produced the best conformations of six molecules, with main hydrogen interactions occurring with residues Gly82, Asp83, Phe84, Asp129, Tyr130, Pro131, Ser135, Tyr150, Asn152, Gly153, Val155, and Tyr161 (Table 5 and Figure S1, Supplementary Information (SI) section). Notably, the residues Phe84, Asp83, Asp129, Asn152, Gly153 and Tyr161 also form hydrogen bonds with the reference crystal inhibitor in the enzyme complex's active site, as shown in Figure 4. These findings suggest that the conformations obtained by the programs are similar to the reference ligand in the active site of NS2B-NS3 protease.

Figure 5 depicts the optimal conformations obtained by the docking algorithms after refinement using PM7. As shown, all conformations occupy a specific region with clearly defined ring orientations (in the case of flavonoids). The selection of the lowest energy values was used to determine the optimal conformations.

#### Consensual analysis

Consensual docking has been a successful approach in drug discovery, combining the results of different docking programs to increase the accuracy and reliability of the

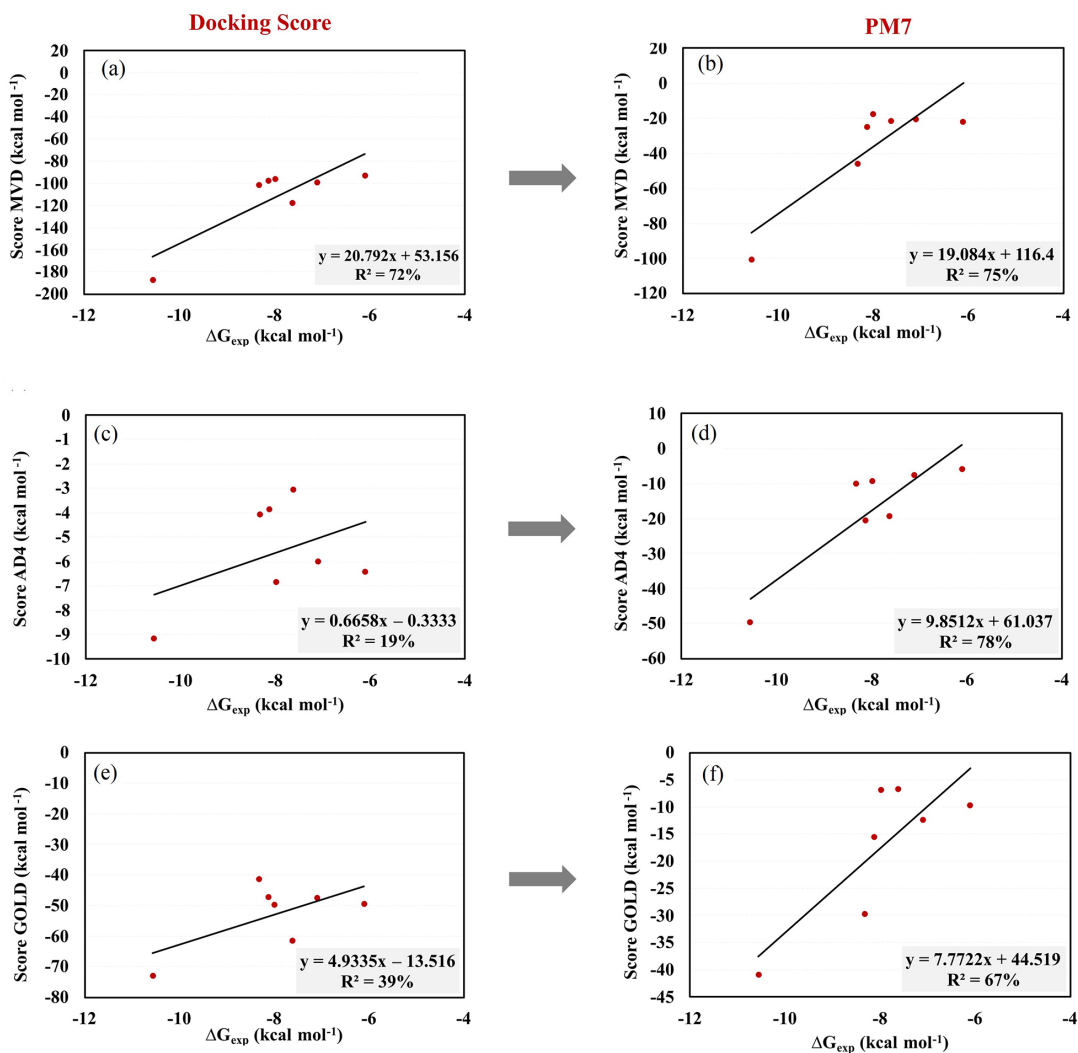


**Figure 3.** Linear regression of experimental values<sup>7</sup> vs. energy values (score) obtained by molecular docking for (a) MVD, (c) AD4 and (e) GOLD program and optimized by the PM7 semiempirical method for (b) MVD, (d) AD4 and (f) GOLD.  $R^2$  values are expressed in percentage to assess reproducibility.

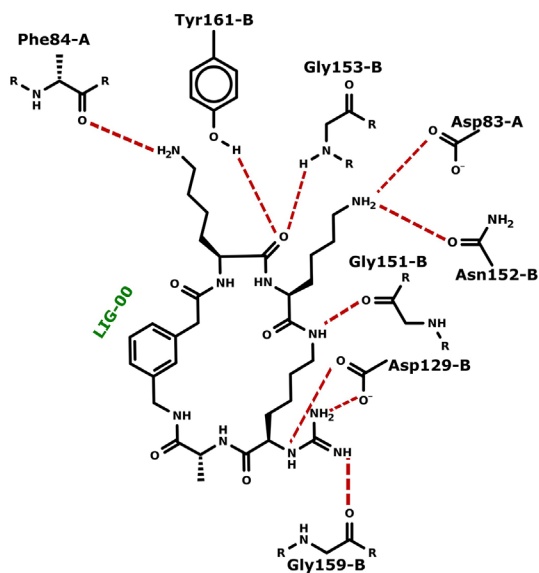


**Figure 4.** The 2D-diagram intermolecular interactions with the reference inhibitor LIG-00.

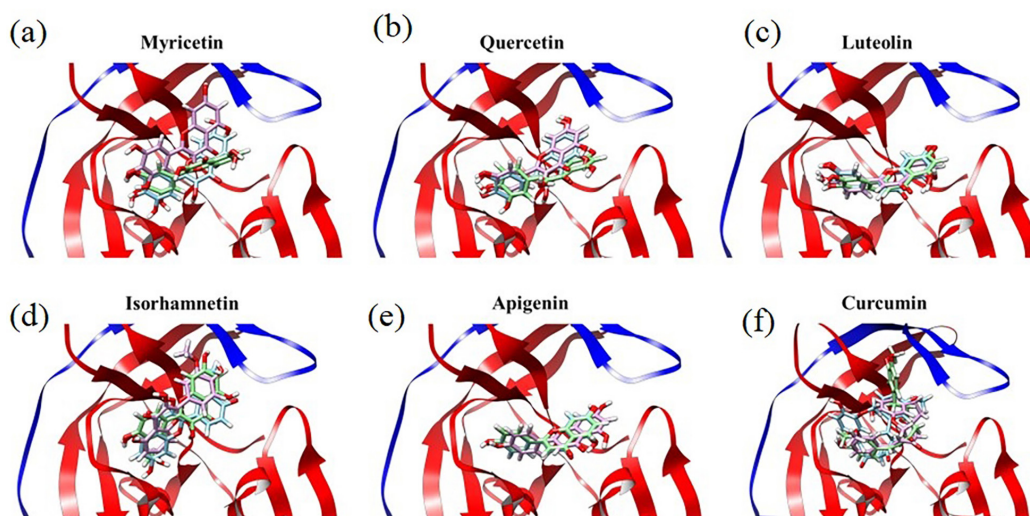
results<sup>17,18</sup> which is considered a valuable tool in drug design and development. Herein, we used the recalculated PM7 energies for the consensual analysis. The energies from structures obtained using GOLD program were excluded from the final ranking ( $F_r$ ) calculations due to the low  $R^2$  values obtained in the linear regression analysis (67%, Figure 3). The results are presented in Table 6, revealing myricetin as the top-ranked ligand with a score of 1.28, followed closely by quercetin (score of 1.26). These findings are in agreement with the experimental data,<sup>7</sup> where ligands 01 and 02 (myricetin and luteolin, respectively) exhibit the lowest  $K_i$  values ( $0.8 \pm 0.1$  and  $1.1 \pm 0.1$   $\mu\text{M}$ , respectively). Table 6 displays the consensual docking results, with a focus on the ligands with the highest final ranking and the lowest binding energies.

Myricetin, with a  $K_i$  value lower than that of all other natural edible plant molecules (shown in Table 2), had the highest  $F_r$  value (1.28). This is consistent with a previous

**Table 5.** Main residues responsible for hydrogen interactions obtained by docking methods

Ligand ID	Docking software		
	MVD	AD4	GOLD
01	Gly153, Ser135 and Tyr130	Phe84, Tyr130 and Asn152	Tyr130, Ser135 and Asn152
02	Gly153, Ser135 and Tyr130	Phe84, Tyr130, Tyr150 and Gly153	Tyr130 and Asn152
03	Asp129, Asn152 and Tyr130	Asp129, Tyr130 and Tyr150	Tyr130 and Asn152
04	Pro131 and Tyr130	<sup>a</sup>	Asp83, Phe84 and Tyr130
05	Tyr130, Tyr150 and Asn152	Tyr150 and Asp83	Tyr130 and Asn152
06	Gly153	Gly153	Gly82, Asp129, Tyr130, Gly153, Val155 and Tyr161

<sup>a</sup>It does not perform interactions. MVD: Molegro Virtual Docking; AD4: AutoDock 4; GOLD: CSD-GOLD.

**Figure 5.** Best conformations obtained by docking programs (MVD: blue, AD4: lilac, GOLD: green).**Table 6.** Consensual docking results, with emphasis on the results of the highest final ranking ( $F_r$ ) and lowest binding energies,  $\Delta G_{\text{exp}}$ 

Ligand ID	Usual name	$\Delta G_{\text{exp}}^a /$ (kcal mol <sup>-1</sup> )	Final ranking ( $F_r$ )
01	myricetin	-8.32	1.28
02	quercetin	-8.13	1.26
03	luteolin	-7.99	0.23
04	isorhamnetin	-7.10	0.22
05	apigenin	-6.10	0.16
06	curcumin	-7.62	1.05

<sup>a</sup>Binding energy value obtained experimentally by literature.

study<sup>33</sup> that also evaluated the ZIKV NS2B-NS3Pro complex and observed myricetin as having the lowest  $K_i$  ( $8.9 \pm 1.9 \mu\text{M}$ ) among other molecules such as rutin, astragalín, and quercetin. It is important to note that quercetin presented the second highest final ranking in the present work after optimization by PM7. Myricetin is a flavonoid with promising research on its therapeutic effect on various diseases, including inflammatory diseases,<sup>34-36</sup> anticancer,<sup>37</sup> thrombosis (anticoagulant),<sup>38,39</sup> diabetes,<sup>40</sup>

Alzheimer's disease<sup>41</sup> and others.<sup>42</sup> Therefore, research on natural products derived from edible plants is important as a single product can have several therapeutic effects, making it a good candidate for a multi-target inhibitor. Furthermore, the consistent results obtained from the association of the molecular docking method and the PM7 semi-empirical method with the literature indicate their potential for future studies to screen new molecules, particularly, natural compounds.

## Conclusions

Combining molecular docking with semi-empirical methods can improve the accuracy of predicting ligand-protein interactions. In this study, redocking validated the reliability of the molecular docking results to generate poses, and the PM7 semi-empirical method improved the energies correlation in MVD, AD4, and GOLD results. The use of MVD, followed by optimization with the PM7 method was found to be the most accurate tool for determining binding energies for the class of ligands studied. The natural compound myricetin was found to

have the best value (1.28), which is in agreement with the lowest  $\Delta G_{\text{bind,exp}}$  ( $-8.32 \text{ kcal mol}^{-1}$ ) observed among the compounds studied here. Overall, these results demonstrate the effectiveness of combining molecular docking and semiempirical methods for refining docking results and identifying potential Zika Virus NS2B-NS3 protease inhibitors.

## Supplementary Information

Supplementary information is available free of charge at <http://jbcs.s bq.br> as PDF file.

## Acknowledgments

We would like to thank Fundação Amazônia de Amparo a Estudos (FAPESPA) and Conselho Nacional de Desenvolvimento Científico e Tecnológico (CNPq) for funding our research under Chamada No. 002/2021-Programa de Infraestrutura para Jovens Pesquisadores-Programa Primeiros Projetos-PPP-FAPESPA/CNPq.

## References

- D'Ortenzio, E.; Matheron, S.; de Lamballerie, X.; Hubert, B.; Piorkowski, G.; Maquart, M.; Descamps, D.; Damond, F.; Yazdanpanah, Y.; Leparç-Goffart, I.; *N. Engl. J. Med.* **2016**, *374*, 2195. [Crossref]
- Mlakar, J.; Korva, M.; Tul, N.; Popović, M.; Poljšak-Prijatelj, M.; Mraz, J.; Kolenc, M.; Resman Rus, K.; Vesnaver Vipotnik, T.; Fabjan Vodušek, V.; Vizjak, A.; Pižem, J.; Petrovec, M.; Avšič Županc, T.; *N. Engl. J. Med.* **2016**, *374*, 951. [Crossref]
- e Silva, A. L. P.; Spalding, S. M.; *Rev. Médica de Minas Gerais* **2018**, *28*, e-1933. [Crossref]
- Huber, S.; Braun, N. J.; Schmacke, L. C.; Quek, J. P.; Murra, R.; Bender, D.; Hildt, E.; Luo, D.; Heine, A.; Steinmetzer, T.; *J. Med. Chem.* **2022**, *65*, 6555. [Crossref]
- Katzelnick, L. C.; Narvaez, C.; Arguello, S.; Lopez Mercado, B.; Collado, D.; Ampie, O.; Elizondo, D.; Miranda, T.; Bustos Carillo, F.; Mercado, J. C.; Latta, K.; Schiller, A.; Segovia-Chumbez, B.; Ojeda, S.; Sanchez, N.; Plazaola, M.; Coloma, J.; Halloran, M. E.; Premkumar, L.; Gordon, A.; Narvaez, F.; de Silva, A. M.; Kuan, G.; Balmaseda, A.; Harris, E.; *Science* **2020**, *369*, 1123. [Crossref]
- da Silva, S. R.; Gao, S.-J.; *J. Med. Virol.* **2016**, *88*, 1291. [Crossref]
- Roy, A.; Lim, L.; Srivastava, S.; Lu, Y.; Song, J.; *PLoS One* **2017**, *12*, e0180632. [Crossref]
- Braun, N. J.; Quek, J. P.; Huber, S.; Kouretova, J.; Rogge, D.; Lang-Henkel, H.; Cheong, E. Z. K.; Chew, B. L. A.; Heine, A.; Luo, D.; Steinmetzer, T.; *ChemMedChem* **2020**, *15*, 1439. [Crossref]
- Santana, K.; do Nascimento, L. D.; Lima e Lima, A.; Damasceno, V.; Nahum, C.; Braga, R. C.; Lameira, J.; *Front. Chem.* **2021**, *9*, 662688. [Crossref]
- Berman, H. M.; Westbrook, J.; Feng, Z.; Gilliland, G.; Bhat, T. N.; Weissig, H.; Shindyalov, I. N.; Bourne, P. E.; *Nucleic Acids Res.* **2000**, *28*, 235. [Crossref]
- Pettersen, E. F.; Goddard, T. D.; Huang, C. C.; Couch, G. S.; Greenblatt, D. M.; Meng, E. C.; Ferrin, T. E.; *J. Comput. Chem.* **2004**, *25*, 1605. [Crossref]
- Frisch, M. J.; Trucks, G. W.; Schlegel, H. B.; Scuseria, G. E.; Robb, M. A.; Cheeseman, J. R.; Scalmani, G.; Barone, V.; Mennucci, B.; Petersson, G. A.; Nakatsuji, H.; Caricato, M.; Li, X.; Hratchian, H. P.; Izmaylov, A. F.; Bloino, J.; Zheng, G.; Sonnenberg, J. L.; Hada, M.; Ehara, M.; Toyota, K.; Fukuda, R.; Hasegawa, J.; Ishida, M.; Nakajima, T.; Honda, Y.; Kitao, O.; Nakai, H.; Vreven, T.; Montgomery Jr., J. A.; Peralta, J. E.; Ogliaro, F.; Bearpark, M.; Heyd, J. J.; Brothers, E.; Kudin, K. N.; Staroverov, V. N.; Kobayashi, R.; Normand, J.; Raghavachari, K.; Rendell, A.; Burant, J. C.; Iyengar, S. S.; Tomasi, J.; Cossi, M.; Rega, N.; Millam, N. J.; Klene, M.; Knox, J. E.; Cross, J. B.; Bakken, V.; Adamo, C.; Jaramillo, J.; Gomperts, R.; Stratmann, R. E.; Yazyev, O.; Austin, A. J.; Cammi, R.; Pomelli, C.; Ochterski, J. W.; Martin, R. L.; Morokuma, K.; Zakrzewski, V. G.; Voth, G. A.; Salvador, P.; Dannenberg, J. J.; Dapprich, S.; Daniels, A. D.; Farkas, Ö.; Foresman, J. B.; Ortiz, J. V.; Cioslowski, J.; Fox, D. J.; *Gaussian 09*, Rev A.02; Gaussian, Inc., Wallingford, CT, 2009.
- Anandakrishnan, R.; Aguilar, B.; Onufriev, A. V.; *Nucleic Acids Res.* **2012**, *40*, W537. [Crossref]
- Thomsen, R.; Christensen, M. H.; *J. Med. Chem.* **2006**, *49*, 3315. [Crossref]
- Morris, G. M.; Huey, R.; Lindstrom, W.; Sanner, M. F.; Belew, R. K.; Goodsell, D. S.; Olson, A. J.; *J. Comput. Chem.* **2009**, *30*, 2785. [Crossref]
- Jones, G.; Willett, P.; Glen, R. C.; Leach, A. R.; Taylor, R.; *J. Mol. Biol.* **1997**, *267*, 727. [Crossref]
- de Oliveira, M. D.; de Araújo, J. O.; Galúcio, J. M. P.; Santana, K.; Lima, A. H.; *J. Mol. Graphics Modell.* **2020**, *101*, 107735. [Crossref]
- de Oliveira, M. V. D.; Bittencourt Fernandes, G. M.; da Costa, K. S.; Vakal, S.; Lima, A. H.; *RSC Adv.* **2022**, *12*, 18834. [Crossref]
- Araújo, J. O.; dos Santos, A. M.; Lameira, J.; Alves, C. N.; Lima, A. H.; *Molecules* **2019**, *24*, 2370. [Crossref]
- Stewart, J. J. P.; *MOPAC2016*; Stewart Computational Chemistry, Colorado Springs, CO, USA, 2016. [Link] accessed in July 2023
- Stewart, J. J. P.; *Int. J. Quantum Chem.* **1996**, *58*, 133. [Crossref]
- Stewart, J. J. P.; *J. Mol. Model.* **2013**, *19*, 1. [Crossref]

23. Stewart, J. J. P.; *J. Mol. Model.* **2007**, *13*, 1173. [Crossref]
24. Sulimov, A. V.; Kutov, D. C.; Katkova, E. V.; Sulimov, V. B.; *Adv. Bioinformatics* **2017**, *2017*, ID 7167691. [Crossref]
25. Moubock, A. F. A.; Li, J.; Mishra, P.; Gao, M.; Günther, S.; *Comput. Struct. Biotechnol. J.* **2019**, *17*, 1367. [Crossref]
26. Temml, V.; Schuster, D. In *Molecular Docking for Computer-Aided Drug Design*; Coumar, M. S., ed.; Elsevier, 2021, p. 391. [Crossref]
27. Bikadi, Z.; Hazai, E.; *J. Cheminform.* **2009**, *1*, 15. [Crossref]
28. Rocha, S. F. L. S.; Sant'Anna, C. M. R.; *Biopolymers* **2019**, *110*, e23320. [Crossref]
29. Schöning-Stierand, K.; Diedrich, K.; Fährrolfes, R.; Flachsenberg, F.; Meyder, A.; Nittinger, E.; Steinegger, R.; Rarey, M.; *Nucleic Acids Res.* **2020**, *48*, W48. [Crossref]
30. Fährrolfes, R.; Bietz, S.; Flachsenberg, F.; Meyder, A.; Nittinger, E.; Otto, T.; Volkamer, A.; Rarey, M.; *Nucleic Acids Res.* **2017**, *45*, W337. [Crossref]
31. Stierand, K.; Maass, P. C.; Rarey, M.; *Bioinformatics* **2006**, *22*, 1710. [Crossref]
32. Fricker, P. C.; Gastreich, M.; Rarey, M.; *J. Chem. Inf. Comput. Sci.* **2004**, *44*, 1065. [Crossref]
33. Lim, H.; Nguyen, T. T. H.; Kim, N. M.; Park, J.-S.; Jang, T.-S.; Kim, D.; *Biotechnol. Lett.* **2017**, *39*, 415. [Crossref]
34. Chen, M.; Chen, Z.; Huang, D.; Sun, C.; Xie, J.; Chen, T.; Zhao, X.; Huang, Y.; Li, D.; Wu, B.; Wu, D.; *Pulm. Pharmacol. Ther.* **2020**, *65*, 102000. [Crossref]
35. Wang, S.-J.; Tong, Y.; Lu, S.; Yang, R.; Liao, X.; Xu, Y.-F.; Li, X.; *Planta Med.* **2010**, *76*, 1492. [Crossref]
36. Jang, J.-H.; Lee, S. H.; Jung, K.; Yoo, H.; Park, G.; *Brain Sci.* **2020**, *10*, 32. [Crossref]
37. Devi, K. P.; Rajavel, T.; Habtemariam, S.; Nabavi, S. F.; Nabavi, S. M.; *Life Sci.* **2015**, *142*, 19. [Crossref]
38. Tan, J.-Y.; Chen, X.-Q.; Kang, B.-J.; Qin, Z.-X.; Chen, J.-H.; Hu, R.-D.; Wu, L.-C.; *Asian Pac. J. Trop. Med.* **2018**, *11*, 255. [Link] accessed in July 2023
39. Gaspar, R. S.; da Silva, S. A.; Stapleton, J.; Fontelles, J. L. L.; Sousa, H. R.; Chagas, V. T.; Alsufyani, S.; Trostchansky, A.; Gibbins, J. M.; Paes, A. M. A.; *Front. Pharmacol.* **2020**, *10*, 1678. [Crossref]
40. Li, Y.; Ding, Y.; *Food Sci. Hum. Wellness* **2012**, *1*, 19. [Crossref]
41. Liu, M.; Guo, H.; Li, Z.; Zhang, C.; Zhang, X.; Cui, Q.; Tian, J.; *Front. Aging Neurosci.* **2020**, *12*, 601603. [Crossref]
42. Song, X.; Tan, L.; Wang, M.; Ren, C.; Guo, C.; Yang, B.; Ren, Y.; Cao, Z.; Li, Y.; Pei, J.; *Biomed. Pharmacother.* **2021**, *134*, 111017. [Crossref]

Submitted: March 23, 2023

Published online: August 7, 2023